PHYSICAL REVIEW B **83**, 165111 (2011)

Density functional theory investigations of the structural and electronic properties of $Ag_2V_4O_{11}$

Maricarmen Grisolía,[1,2] Patrick Rozier,[1] and Magali Benoit[1]
[1]*CEMES UPR 8011, 29 rue Jeanne Marvig, F-31055 Toulouse Cedex, France*
[2]*Grupo de Procesos Dinámicos en Química, Universidad de Los Andes. La Hechicera, Mérida–5101, Venezuela*
(Received 5 November 2010; revised manuscript received 26 January 2011; published 14 April 2011)

We present Density Functional Theory (DFT) investigations in the General Gradient Approximation (GGA) of the structural and electronic properties of the $Ag_2V_4O_{11}$ (SVO) compound. We carried out a detailed study of the different structures of SVO proposed in the literature, by comparing the results obtained using DFT and the DFT+U approach. We found that two of the proposed structures are equally probable, the third one being unstable. We have obtained detailed information concerning the structural and electronic properties of SVO, including previously non-existent information on one of the SVO structures, considered hypothetical yet probable in the light of experimental facts from analogous compounds. From the analysis of the electronic density of states and of the Highest Occupied Molecular Orbital (HOMO) and Lowest Unoccupied Molecular Orbital (LUMO) states, we propose that, during the earlier stage of the reaction of lithium insertion and de-insertion in Li/SVO primary batteries, the reduction of V^{5+} takes place before that of Ag. In addition, our results allow to predict that only one kind of vanadium atom would be firstly reduced.

DOI: 10.1103/PhysRevB.83.165111 PACS number(s): 71.15.Nc, 82.47.Aa, 61.66.Fn

I. INTRODUCTION

The V^{5+}/V^{4+} couple exhibits a high redox potential with respect to lithium.[1] Therefore, lithium batteries, in which the positive electrode contains V^{5+} ions, are very powerful. In vanadium oxides, V^{5+} or a mixture of V^{5+}/V^{4+} is present, making them good industrial candidates for their electrochemical properties. Among these oxides, silver vanadium oxide $Ag_2V_4O_{11}$ (SVO) is commonly used as a cathode for high-rate primary power sources in Implantable Cardioverter Defibrillators (ICD), thanks to its excellent electrochemical performances.[2,3] Li/SVO batteries have a high capacity (between 260 and 360 mAh/g[4–8] for $Li_xAg_2V_4O_{11}$ with a maximum of x equal to 7) and are stable in the long term.[9]

Because of its industrial interest, several experimental studies dealing with the synthesis routes of SVO have been published.[5,6,10] Indeed the electrochemical performance of the compound depends on the synthesis method[9] and is strongly related to its composition and its structural characteristics.[4]

The crystallographic structure of $Ag_2V_4O_{11}$ was resolved by Zandbergen *et al.*[11] using high-resolution electronic microscopy and x-ray diffraction (XRD) spectroscopy. These authors have identified two phases of SVO, both made of $[V_4O_{11}]_n$ layers in the xy plane (perpendicular to the **c** cell parameter). Both structures (structure I and structure II, Table I) can be differentiated by the arrangement of the layers along the **c** direction. The crystallographic structure of structure II is very similar to that of $Cu_{1.8}V_4O_{11}$.[12] It should be mentioned that the existence of structure II has only been evidenced in Ref. 11, in 1994. A third structure (named here structure I'), which differs from structure I only by the length of the cell parameter **a**, has also been reported by Zandbergen *et al.*[11] but has not been observed by others.

The layered structure of SVO makes this compound particularly suited for the intercalation or insertion of Li ions, which enters the structure by occupying the empty sites in the interlayer space. However, the exact positions of the lithium sites as well as the electrochemical mechanism of the reaction are not yet fully understood. Globally, the electrochemical reduction of SVO combined with the lithium discharge in the anode can be represented by the equation[5]:

$$x\mathrm{Li}^+ + \mathrm{Ag}_2\mathrm{V}_4\mathrm{O}_{11} \rightarrow \mathrm{Li}_x\mathrm{Ag}_2\mathrm{V}_4\mathrm{O}_{11}$$

This reaction is often described as taking place in at least three steps[4]:

(1) For $0 < x < 2.4$, silver reduction dominates, with a simultaneous reduction of V^{5+}. During this step, the system can be described as a mixture of $Li_2V_4O_{11}$ and Ag^0 at $x \approx 2$.

(2) For $2.4 < x < 3.8$, the reaction is exclusively the reduction of V^{5+} in V^{4+}.

(3) Beyond $x = 3.8$, vanadium reduction continues and it can be found in its different oxidation states (V^{5+}, V^{4+}, V^{3+}).

In the works of Leising *et al.*[4] and of Crespi *et al.*,[14] silver reduction is the first step of the reaction inside the battery, with the insertion of lithium ions in place of silver ions. However a more recent study, by Sauvage *et al.* in 2010,[15] contradicts this idea. Sauvage *et al.*[15] have performed XRD measurements, combined with electron-spin resonance (ESR) spectroscopy during the reactions of lithium insertion and deinsertion in Li/SVO batteries in order to study the V^{5+} reduction. They found that, in the earlier stage of the reaction, lithium ions are inserted in the intersticial positions in the layered structure during the V^{5+} to V^{4+} reduction. The displacement reaction of silver by lithium starts only from $x \approx 1$. Thus Sauvage *et al.* propose the following steps for the reaction inside the battery:

(1) For $0 < x <\sim 0.7$, there is reduction of V^{5+} without direct evidence of silver extrusion.

(2) For $\sim 0.7 < x <\sim 5.5$, the Ag+/Li+ displacement reaction begins and competes with the V^{5+}reduction reaction.

(3) For $x >\sim 5.5$, the reduction of V^{5+} to V^{4+} and the successive reduction of V^{4+} to V^{3+} are dominant.

It is then clear that the mechanism of this redox reaction is far from being completely understood.

In this paper, we present a detailed theoretical investigation of the electronic and structural properties of $Ag_2V_4O_{11}$ carried out by means of Density Functional Theory (DFT)[16,17] calculations in the gradient corrected approximation[18] and

TABLE I. Experimental structural parameters of $Ag_2V_4O_{11}$.

	Structure I[11,13]	Structure I'[11]	Structure II[11,12]
V [Å^3]	412.23	387.14	396.65
a [Å]	15.48	14.51	15.31
b [Å]	3.58	3.58	3.61
c [Å]	9.54	9.56	7.34
β [°]	128.7	128.7	101.8

by means of the DFT + U approach[19] in order to evaluate the possible electronic correlation effects in this system. After a validation of the employed methods on the V_2O_5 system, we present an analysis of the system size effects on the structural and electronic characteristics of $Ag_2V_4O_{11}$. Then we investigate the effect of the DFT + U correction on this compound. Finally, a discussion on the different phases proposed in the literature for the $Ag_2V_4O_{11}$ system is given and a possible mechanism for the reaction of this compound with respect to lithium is suggested.

II. SIMULATION DETAILS

The $Ag_2V_4O_{11}$ system has been studied by means of Density Functional Theory (DFT)[16,17] calculations based on the gradient corrected PBE functional[18] for the exchange and correlation energy. Calculations have been carried out using the QUICKSTEP module[20] of the CP2K code.[21,22] The wavefunctions were developed on Gaussian basis functions of the DZBP type[23] for V, O and Ag and an auxiliary basis of plane waves with an energy cutoff E_{cut} was used for the density matrix. Only the Γ point was used for the Brillouin zone sampling but, as explained later, calculations on different cell sizes were carried out in order to check the effect of this approximation.

Pseudopotentials developed by Goedecker *et al.*[24] have been used for the three atomic species. For vanadium, only the $3s3p4s3d$ states have been explicitly considered, for silver only the $5s4d$ states, and for oxygen the $2s2p$ states. The basis sets, as well as the pseudopotentials and the functional, have been tested on simple systems and molecules.

First, full cell relaxations have been carried out on the V_2O_5 system for a cell size $1 \times 3 \times 3$ times the 14-atoms unit cell. The convergency of the results with respect to the number of plane waves (cutoff energy, E_{cut}) has been studied. We have also compared the results with those of calculations performed with a converged number of k points in the Brillouin zone with the VASP code.[25–28] In V_2O_5, the vanadium ions are located in square pyramidal environments, which can be considered as distorted octahedron with a short V–O vanadyl bond (1.577 Å), four longer V–O bonds, and one very long V–O distance (2.791 Å) which corresponds to the distance between layers and is actually not considered as a real bond.

The results presented in Table II were obtained with high cutoff energies with VASP (900 eV) as well as with CP2K (1000 Ry for the density, i.e., 250 Ry). For V_2O_5, the dependency of the cell parameters and V–O distances with the energy cutoff is particularly important for the **c** parameter and the interlayer distance. From Table II, one can note that the results obtained for the $1 \times 3 \times 3$ cell box

TABLE II. Structural parameters for V_2O_5 and the Ag–O molecule, calculated using CP2K and compared with experimental values and VASP calculations. VASP calculations have been carried out with PAW pseudopotentials for O ($2s2p$ states) and V ($3p4s3d$ states), in the PBE[18] approximation with a cutoff energy of $E_{cut} = 900$ eV and a $4 \times 6 \times 6$ k-points grid.

	V_2O_5			
	This work			
	VASP	CP2K	CP2K (DFT-D)	Exp.[29]
V [Å^3]	199.24	196.01	185.39	179.3
a [Å]	11.562	11.520	11.582	11.512
b [Å]	3.576	3.574	3.544	3.564
c [Å]	4.819	4.760	4.517	4.371
V–O(1) [Å]	1.599	1.584	1.586	1.577
V–O(2) [Å]	1.795	1.790	1.785	1.779
V–O(3) [Å]	1.893	1.891	1.881	1.878
V–O(3') [Å]	2.045	2.041	2.057	2.017
V–O_{next} [Å]	3.221	3.177	2.931	2.791
Gap [eV]	2.25	2.01	1.99	2.30[30] 2.38[31]
	AgO molecule			
	This work (CP2K)			Exp.[32]
Ag–O [Å]	2.0055			2.0056

are comparable to those obtained using the VASP code with a fully converged k-points calculation. For the $1 \times 3 \times 3$ cell box with CP2K , there is an overall good agreement between the calculated volume, cell parameters and V–O distances and the experimental data, except for the **c** parameter and the long V–O distance which are largely overestimated.

Previous calculations carried out on this system have shown large variations on these two structural characteristics which, in some cases, are due to nonconverged calculations.[1,33,34] These large variations are due to the fact that present DFT methods cannot properly account for weak van der Waals interactions between the layers in V_2O_5. Indeed, converged calculations give an interlayer distance between 13% and 15% larger than the experimental one, both with VASP and CP2K .

As already proposed by Kerber *et al.*,[35] if we include a semiempirical correction of the dispersion, such as the DFT-D proposed by Grimme,[36] the description of the interaction between layers—and thus the interlayer distance and the **c** parameter—is significantly improved (Table II). This result has been more recently confirmed and explained in detail by Londero and Schröder[37] who studied the role of the van der Waals bonding in V_2O_5 by means of the vdW-DF method.[38]

The direct gap is found to be in good agreement with the experimental gap, even if it is a well-known fact that DFT fails in providing correct electronic gaps. The better value obtained with VASP compared to CP2K can be explained by the use of a converged k-point grid in the VASP calculation.

Finally, we computed the equilibrium distance in the Ag-O molecule with CP2K (Table II), in order to check the Ag pseudopotential and basis, and we obtained a very good agreement with experiments.

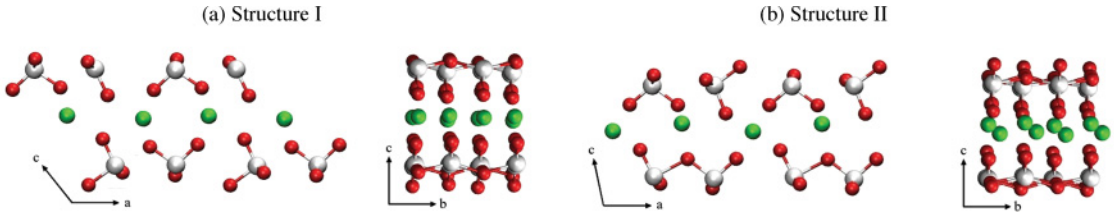

FIG. 1. (Color online) Structures I (a) and II (b) of $Ag_2V_4O_{11}$ (SVO), projected on the *ac* (left) and the *bc* (right) planes. The vanadium, oxygen, and silver atoms are depicted in white, black, and grey (grey, red, and green online), respectively. The silver atoms lie in channels perpendicular to the figure plane.

For the simulations of $Ag_2V_4O_{11}$, we will use CP2K with an energy cutoff of 600 Ry for the electronic density, for which a good convergency of the structural characteristics of the system has been obtained. For this compound we did not use the dispersion correction since the problem of weak interactions between the layers should not be present due to the presence of Ag atoms located in channels between the layers.

III. RESULTS

In the three proposed $Ag_2V_4O_{11}$ structures (Fig. 1), each vanadium ion in the $[V_4O_{11}]_n$ layers is surrounded by six oxygen atoms, forming a distorted octahedron. The SVO structure is thus composed of VO_6 octahedra connected by edges and corners, building up the $[V_4O_{11}]_n$ layers in the *ab* plane. The V(1) octahedra share three edges and one corner and the V(2) octahedra share five edges (Fig. 2), each vanadium atom having one oxygen ligand (the vanadyl oxygen, V = O), which is not shared with any other V atom.[39] The oxygen atoms are classified following their number of bonds with the vanadium atoms: O1 corresponds to the unshared octahedra corner, and the other oxygen atoms are bridging oxygens. The V1–O2′ and V2–O4′ bonds are longer than the corresponding V1–O2 and V2–O4 ones. The V1 and V2 atoms share the O2′, O3, and O4 oxygen atoms. The bond with O1 is the shortest one since it is a vanadyl type bond (V = O).

The silver atoms occupy interlayer sites, located between the vanadyl oxygens, forming channels along the **b** direction. The environment of the silver atoms is quite different in the three structures: In structures I and I', all Ag atoms have five oxygen neighbors in a coordination sphere of 2.8 Å which, extended to about 3.2 Å, leads to seven oxygen neighbors with an environment that can be described as a monocapped trigonal prism, whereas in structure II, two different types of Ag atoms exist, one with four oxygen neighbors and one with six in a 2.8 Å coordination sphere.

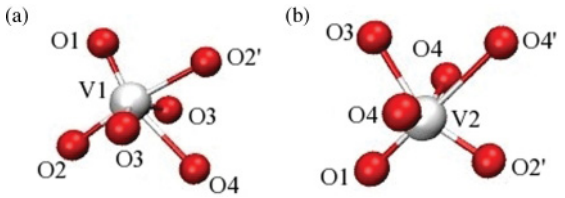

FIG. 2. (Color online) Environments of the V1 (a) and V2 (b) vanadium atoms in SVO.

A. System size effects

The choice of the CP2K code, which includes only the Γ point for the Brillouin-zone sampling, makes necessary the use of a supercell. In order to ensure the convergency of the results with respect to the supercell size and to take into account possible anisotropy effects on the geometric and electronic characteristics of the system, we have carried out cell optimizations for several supercell sizes of $Ag_2V_4O_{11}$, structure I. These tests will also be useful for future simulations of non-stoichiometric SVO[40] which can be obtained due to oxygen deficiencies ($Ag_2V_4O_{11-y}$)[41] or silver deficiencies ($Ag_{2-x}V_4O_{11}$),[11] or when the insertion of small percentages of lithium atoms are considered.

By testing the supercell size, we also intend to evaluate the relative importance of the interatomic interactions of specific spatial orientations. It is important as well to take into account a possible delocalization of the Ag ions during the electrochemical reaction. Indeed, in the $Cu_{7/3}V_4O_{11}$ compound, a superstructure which is obtained by multiplying the **b** cell parameter by 9 has been reported[12] in which the Cu atoms are delocalized in channels parallel to **b** and for which a high reactivity with respect to lithium has been observed.[42]

The size effects on the geometrical and electronic characteristics of $Ag_2V_4O_{11}$ have therefore been investigated by multiplying the 34-atoms unit cell along the **b** axis and **c** axis. The results of the cell optimizations for structure I are presented in Table III . They show a significant difference between the experimental cell volume and the calculated one. This difference is mainly due to larger **a** and **c** cell parameters with respect to the experimental ones. The use of larger supercells does not correct for this trend. This result can be related to the overestimation of the cell volume and parameters of the V_2O_5 system presented in Table II due to an inadequate treatment of the long-range electronic correlation, which is a well-known DFT failure.[43,44]

Nevertheless, the evolution of the total energy, total volume, and energy gap, presented in Fig. 3 as a function of the cell size, show interesting trends. The total energy converges for supercells in which **c** is multiplied by two and **b** is multiplied by at least three. However, when the volume and gap are considered, it is necessary to use **b** vectors multiplied by four with respect to the unit cell in order to obtain convergency. In our calculations, we have therefore used a $1 \times 4 \times 2$ supercell of $Ag_2V_4O_{11}$.

B. DFT + U

Electronic structure calculations carried out on different vanadium oxides, among which α'-NaV_2O_5,[45] $Li_xV_6O_{13}$,[46]

TABLE III. Structural and energetic characteristics of $Ag_2V_4O_{11}$ obtained in DFT for different cell sizes. The cell parameters and total energy correspond to the 34-atoms unit cell.

Size	Number of atoms	V [Å^3]	a [Å]	b [Å]	c [Å]	β [°]	E_{tot} [eV]	Gap [eV]
$1\times2\times1$	68	425.63	15.927	3.548	9.608	128.4	−29 233.087	0.930
$1\times2\times2$	136	424.30	15.898	3.552	9.571	128.3	−29 232.973	0.823
$1\times2\times3$	204	425.91	15.967	3.550	9.570	128.3	−29 232.984	0.855
$1\times3\times1$	102	429.15	15.958	3.563	9.623	128.3	−29 232.042	0.939
$1\times3\times2$	204	426.51	15.872	3.569	9.571	128.1	−29 231.898	0.720
$1\times3\times3$	306	429.51	15.975	3.562	9,594	128.1	−29 231.912	0.912
$1\times4\times1$	136	428.85	15.959	3.546	9.664	128.4	−29 232.095	0.801
$1\times4\times2$	272	427.57	15.924	3.554	9.617	128.2	−29 231.981	0.750
$1\times4\times3$	408	427.74	15.929	3.552	9.627	128.2	−29 231.989	0.765
$1\times6\times1$	204	427.60	15.887	3.553	9.655	128.3	−29 232.106	0.793
$1\times6\times2$	408	427.56	15.922	3.554	9.617	128.2	−29 231.988	0.742
$1\times6\times3$	612	427.43	15.911	3.555	9.617	128.2	−29 231.996	0.761

and β-SrV_6O_{15},[47] have focused on the description of the V–O interactions (electron transfer from O 3*p* to V 3*d* orbitals due to the covalent character of the V–O bonds), as well as on the clarification of the valence states of the vanadium atoms in those compounds. Nevertheless, because vanadium *d* orbitals are partially filled, the electronic description of these systems is particularly difficult using traditional DFT methods. Indeed, strong correlation effects might exist as well as quantum spin fluctuations which are not well described by DFT in the GGA approximation. Therefore, calculations in the DFT + U approach[48–51] have been performed for the study of the oxidation reactions of several vanadium oxides,[52] as well as for the study of the lithium intercalation process during the V_2O_5 reduction.[53] In these investigations, the use of the DFT + U scheme has lead to significant improvements on the prediction of the vanadium valence state in these compounds and on its change of oxidation state during the *redox* reactions. Other vanadium oxide compounds have magnetic properties which are not reproduced by traditional DFT methods (α'-NaV_2O_5,[54] β-$Cu_2V_2O_7$,[55] and $CeVO_4$[56]). In these cases, the DFT + U calculations have been able to reproduce the experimental ground-state structural and magnetic properties.

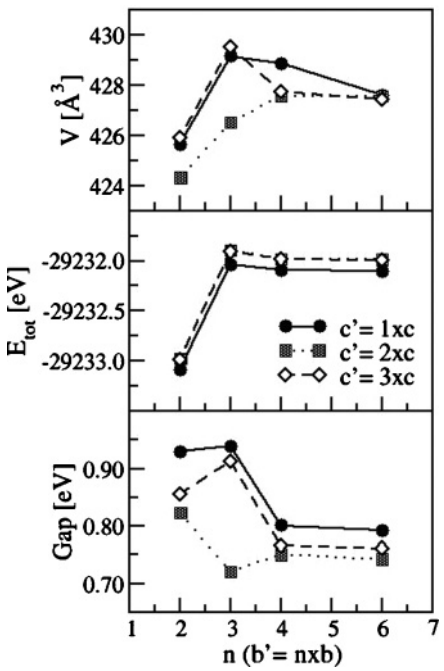

FIG. 3. Evolution of the volume (upper graph), total energy (middle graph), and energy gap (lower graph) as a function of the cell size along **b** for different values of **c**.

In $Ag_2V_4O_{11}$, since the vanadium atoms are supposed to be in their formal V^{5+} oxidation state, we do not expect significant correlation effects. Nevertheless, in the perspective of studying the Li insertion in this compound, for which correlation effects will certainly be significant, we decided to use the DFT + U correction for the study of $Ag_2V_4O_{11}$ system. Within the DFT + U approach, a Hubbard-like term is applied to atom-projected orbitals of interest (here the V 3*d* orbitals), which introduces an energetic penalty to partial occupation. The choice of the value of U_{eff} (=U-J, in the Dudarev formulation[51]) is usually obtained from the reproduction of several experimental features such as the optical band gap, or peak positions in the density of states. The lack of such experimental data for the $Ag_2V_4O_{11}$ compound has lead us to select the value of U_{eff} almost exclusively from geometrical results.

The exchange and correlation energy depends on the representation of the individual particles and, because of this, the value of U_{eff} depends on the choice of the orbitals on which the correction is applied,[57] on the way the orbital occupations are computed,[48] on the chosen L(S)DA + U/GGA + U implementation[58] and on the calculation method (empirical or *ab initio*).[58,59] In the case of calculations performed on vanadium oxides, several values of U_{eff} have been used depending on the chosen approximation and basis set: 3.1 eV for V_2O_5,[52] 1.0 for V_2O_5/TiO_2,[60] and 4.0 eV for $Li_2V_2O_5$[53] in GGA + U with plane augmented waves (PAW), or else 5.9 eV[54] and 3.0 eV[61] for $Na_2V_2O_5$ in LDA + U with linear muffin-tin type orbitals (LMTO). In this context, the optimization of the 272-atoms ($1\times4\times2$) supercell of $Ag_2V_4O_{11}$ (structures I and II) has thus been performed for several values of U_{eff} (Fig. 4) and we have analyzed the variation of the structural and electronic properties of the systems.

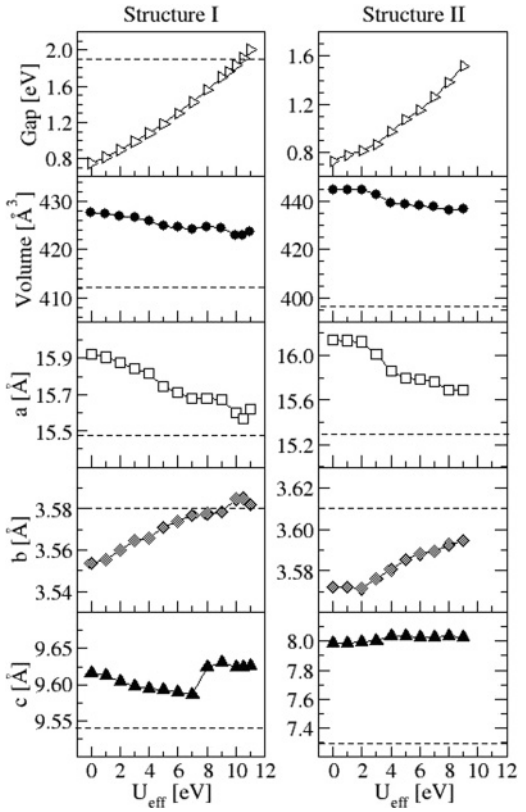

FIG. 4. Evolution of the HOMO-LUMO gap, the cell volume, and the lattice parameters as a function of the value of U_{eff} for a supercell of $1 \times 4 \times 2$ the unit cell (272 atoms) for SVO structures I (left graphs) and II (right graphs). The solid lines are used as guides to the eyes and the dashed lines represent the experimental values from Table I.

From these results, we observe that the DFT + U approach influences both the geometry and the electronic structure of the $Ag_2V_4O_{11}$ system. In particular, the **a** cell parameter is significantly lowered and the band gap is increased. The effects of electronic correlations are therefore not negligible in this system and the use of DFT + U in the subsequent calculations is justified. In the case of structure II, we should recall that the experimental parameters given in Ref. 11 were those of the $Cu_2V_4O_{11}$ compound reported by Galy.[12] A large discrepancy between our results and the experimental values is therefore to be expected. Yet the choice of the best U_{eff} value is not straightforward from these results given the lack of experimental data to compare with. Nevertheless, a value of U_{eff} equal to 7.0 eV seems to give the best agreement with the structural characteristics of the system for both structures I and II. We chose not to adjust the value of U_{eff} to reproduce the electronic gap since this comparison would have been of little relevance here.

At this point it is important to recall that the U_{eff} value is strongly dependent on the specific calculation parameters and implementation, and that no other DFT + U calculations performed with the CP2K code have been reported until now. As we will see next, the differences on the electronic structure of both SVO structures induced by the U_{eff} parameter are not negligible, but they are not determinant for the most important electronic properties of the system. Actually, in our tests

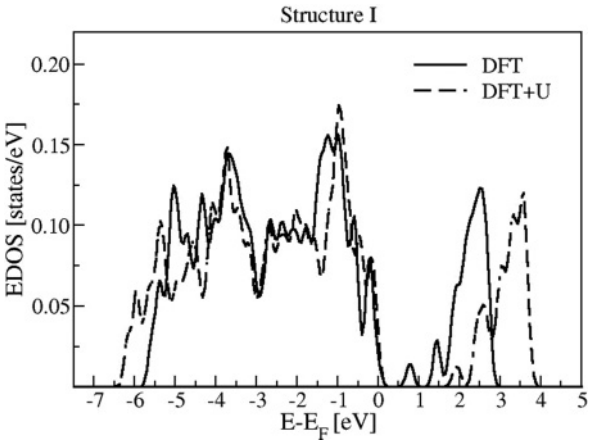

FIG. 5. Kohn-Sham densities of states of SVO, structure I, calculated in DFT and DFT + U (U_{eff} = 7.0 eV).

we have found the effect of the DFT + U correction on the electronic structure of SVO to be very similar for smaller U_{eff} values, with the primary effect for larger U_{eff} values being that of the widening of the band gap. The same is true for the relative stability of the three SVO structures. Also, the choice of a coherent U_{eff} value in our study is important for future calculations to be performed on other vanadium oxide compounds, particularly those involved in the reaction with lithium and others corresponding to mixed Cu/Ag compounds, where the electronic correlation effects might actually be very important. Therefore, our choice of this seemingly large value for U_{eff} that best reproduces the cell parameters for both SVO structures I and II is justified for this system with our calculation setup.

Finally, we analyzed the impact of the Hubbard correction on the Kohn-Sham electronic density of states (EDOS) for structure I of SVO. The EDOS calculated in DFT and DFT + U on the optimized cells are shown in Fig. 5. As we have already mentioned, the major effect of the Hubbard correction is to open the band gap. However one can also observe that the valence band is larger in DFT + U than in DFT and that the main peak at ≈ -1 eV is changed. As we will see later, this peak corresponds mainly to Ag-O hybridization which is weakened when the +U correction is applied.

C. Comparison of the structures I, I', and II

We have then computed the three structures of $Ag_2V_4O_{11}$ proposed in the literature, in the DFT and the DFT + U approximations.

1. Relative stabilities

We first present, in the upper portion of Table IV, the results obtained for geometry optimizations carried out at fixed experimental cells. In that case, structure I appears more stable than structures I' and II by -1.048 eV and -1.811 eV, respectively, in DFT and by -0.948 eV and -1.833 eV, respectively, in DFT+U. Here the DFT + U correction seems to stabilize structure I' and, on the contrary, structure II becomes even less stable, compared to structure I.

Nevertheless, once we let the cell parameters and volume relax, we obtain a completely different scenario, as one can

TABLE IV. Total energies and HOMO-LUMO gap values of the different structures of SVO, computed for the fixed experimental cells in DFT and DFT + U (U_{eff} = 7.0 eV) (upper table), and after cell optimization carried out in DFT and DFT + U (U_{eff} = 7.0 eV) (lower table). The total energies correspond to the 34-atoms unit cell.

Experimental cell			
	DFT		
	Structure I	Structure I'	Structure II
E_{tot} [eV]	−29 231.832	−29 230.784	−29 230.021
Gap [eV]	0.82	0.81	0.60
	DFT + U		
	Structure I	Structure I'	Structure II
E_{tot} [eV]	−29 182.574	−29 181.626	−29 180.741
Gap [eV]	1.34	1.41	0.73

Relaxed cell		
	DFT	
	Structure I	Structure II
E_{tot}[eV]	−29 231.981	−29 232.009
Gap [eV]	0.75	0.73
	DFT + U	
	Structure I	Structure II
E_{tot} [eV]	−29 182.665	−29 182.682
Gap [eV]	1.42	1.26

see in the lower portion of Table IV. First of all, structure I' appears to be unstable and transforms spontaneously into structure I. Secondly, we now observe that structure II has become sligthly more stable than structure I, by an amount of −28 meV in DFT and of −17 meV in DFT+U. After cell optimization, i.e. at equilibrium in our DFT and DFT+U descriptions, we observe an inversion of stability even if the differences in energy are quite small (0.82 meV/at. in DFT and 0.50 meV/at. in DFT+U) which indicates that these two phases would be equally existing. This surprising result is in apparent contradiction with the fact that structure I is the most often observed phase and that structure II has only been observed once.

This inversion of stability when the cell is relaxed is mainly due to large modifications of the cell parameters and volume in the case of structure II as we will see below. Indeed, the total energy of structure I before and after the cell optimization has changed only by −149 meV in DFT and by −91 meV in DFT+U, whereas for structure II this energy change is of −1.988 eV in DFT and of −1.941 eV in DFT+U.

2. *Structural properties*

Let us now analyze the main changes that occurred during the cell optimization for structures I and II. In Table V , the cell volume and parameters are given after optimization of these two systems in DFT and DFT + U. Concerning structure I, the main effect of the cell optimization is to increase the value of **a**, which results in an increase of the cell volume. The **b** and **c** parameters and the β angle are almost unchanged. The DFT + U optimization improves slightly the description of the system with respect to experiment by decreasing the value of **a** with respect to the DFT value. On the other hand, in the case of structure II, the modifications are more substantial. The **a** and **c** parameters and the β angle are quite affected by the cell optimization which leads to a large increase of the cell volume. In DFT + U, we observe the same trend but with a smaller value for **a** and a slightly larger angle. Here we should recall that the experimental parameters given in Ref. 11 were those of the $Cu_2V_4O_{11}$ compound reported by Galy.[12] Therefore, given the difference in atomic size between Cu and Ag, one would expect an increase of the cell volume. However we also observe here a significant shift of the $[V_4O_{11}]_n$ layers with respect to each other which is coherent with the increase of **c**.

Using DFT and DFT + U, we could therefore stabilize a hypothetic structure for $Ag_2V_4O_{11}$, with structural parameters derived from those of $Cu_2V_4O_{11}$. We have checked this result by optimizing the two structures using VASP, with PAW pseudopotentials and a full convergency of the k points and we obtained very similar parameters at equilibrium, with structure II being slightly more stable than structure I, as for the calculations performed with CP2K. Our opinion is then that, even if the existence of such a structure is questionable, it could certainly be obtained using quite specific experimental conditions since it was already observed once. Moreover, recent results[62] report that synthesis of mixed (Cu,Ag)V_2O_5 systems leads to structures always related to pure $Cu_xV_2O_5$ phases despite strong differences with pure $Ag_xV_2O_5$ phases. These experimental facts adapted to similar (Cu,Ag)V_4O_{11} mixed compounds could indicate that their structure would be strongly related to that of the pure $Cu_2V_4O_{11}$ compound. This evidences that $Ag_2V_4O_{11}$ with a structure close to that of $Cu_2V_4O_{11}$ might indeed be stable.

TABLE V. Optimized cell parameters of SVO, structures I and II, in DFT and DFT + U (U_{eff}=7.0 eV).

	Structure I			Structure II		
	Exp[13]	DFT	DFT + U	Exp[11]	DFT	DFT + U
V [Å^3]	412.2	427.6(+3.74%)	424.2(+2.91%)	396.6	444.8(+12.1%)	437.5(+10.31%)
a [Å]	15.480	15.924(+2.87%)	15.680(+1.29%)	15.035	16.139(+7.34%)	15.765(+4.86%)
b [Å]	3.580	3.554(−0.73%)	3.577(−0.08%)	3.610	3.572(+1.05%)	3.590(+0.57%)
c [Å]	9.537	9.616(+0.83%)	9.587(+0.54%)	7.335	7.986(+8.87%)	8.025(+9.41%)
β [degrees]	128.74	128.21(−0.41%)	127.91(−0.64%)	101.84	104.98(+2.99%)	105.56(+3.65%)

TABLE VI. Interatomic distances in structures I and II of SVO, from optimized cell calculations carried out in DFT and DFT + U (U_{eff} =7.0 eV). The atom labels correspond to those defined in Fig. 2. All distances are given in Å.

	Structure I			Structure II		
	Exp[13]	DFT	DFT + U	Exp[a]	DFT	DFT + U
Ag–O	2.3981	2.4114	2.4357	2.1723	2.3892	2.4236
V1–O1	1.6125	1.6166	1.6124	1.6529	1.6324	1.6270
V1–O2	1.8041	1.7908	1.7863	1.7995	1.8044	1.7871
V1–O2’	2.1495	2.2027	2.1386	2.1698	2.3263	2.1516
V1–O3 (×2)	1.8692	1.8741	1.8819	1.8790	1.8772	1.8824
V1–O4	2.2435	2.3203	2.2829	2.2054	2.2289	2.2158
V2–O1	1.6225	1.6468	1.6352	1.6263	1.6437	1.6329
V2–O2’	1.7354	1.7400	1.7420	1.7811	1.7259	1.7307
V2–O3	2.1295	2.1841	2.1182	2.0678	2.1500	2.0956
V2–O4 (×2)	1.8822	1.8746	1.8768	1.8878	1.8875	1.8844
V2–O4’	2.4145	2.5030	2.4746	2.3689	2.7433	2.6068

[a]Because of the lack of precise experimental data for this structure, these distances have been estimated from those of the $Cu_2V_4O_{11}$ compound reported by Galy[12] as suggested in Ref. 11.

In the following, we will analyze the electronic and geometric properties of the two structures of SVO, keeping in mind that the structure II might be that of an hypothetic phase.

In Table VI, the interatomic distances are presented for the two structures I and II, calculated in DFT and DFT + U. Here we will only analyze the agreement of the V–O interatomic distances with experiment for structure I since the experimental distances are not significant for structure II. Overall we can notice a quite good agreement between the computed and measured interatomic V–O distances, the largest discrepancies being obtained for V1–O2’ (+2.47% in DFT and −0.51% in DFT + U), for V1–O4 (+3.42% in DFT and +1.76% in DFT + U), for V2–O3 (+2.56% in DFT and −0.53% in DFT + U), and for V2–O4’ (+3.66% in DFT and +2.45% in DFT + U). These discrepancies are all improved by the use of the Hubbard correction. Also, the structure made of layers connected through channels of Ag ions along the *y* direction is maintained in both cases. The Hubbard correction applied on the 3*d* vanadium orbitals strengthens the V–O interactions which results in a shortening of these bonds with respect to the DFT calculations.

We then observe an overall increase of the Ag–O distances with respect to experiment, which is larger in structure II (+11.57% in DFT + U) than in structure I (+1.57% in DFT + U). In the two structures, the Ag environments are quite different. Actually, in structure II, we find two types of

TABLE VII. Ag–O interatomic distances for structure I, from cell optimization performed in DFT and DFT + U (U_{eff} = 7.0 eV). All distances are given in Å.

	Exp[13]	DFT	DFT + U
Ag–O(1)	2.341	2.341	2.332
Ag–O(2)	2.391 (×2)	–	–
Ag–O(3)	2.453 (×2)	2.429 (×4)	2.462 (×4)

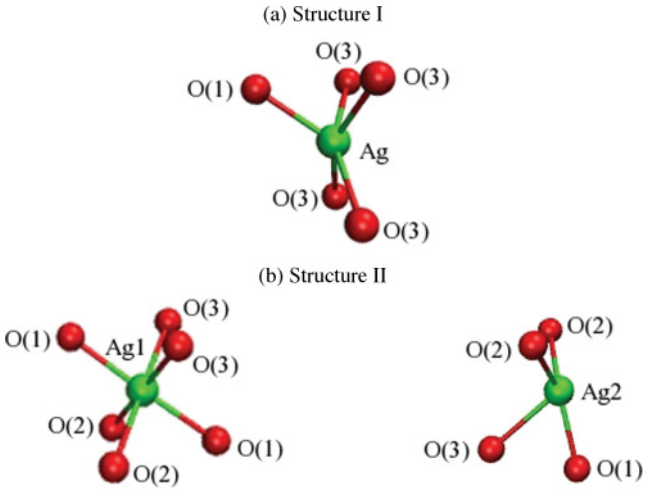

FIG. 6. (Color online) Environments of the silver atoms in the optimized cell, using DFT + U, for structures I (a) and II (b). The oxygen labels correspond to that given in Tables VII and VII.

silver atoms which are bonded to a different number of oxygen atoms. Moreover, these environments are different when they are computed in DFT or DFT + U.

In structure I (Table VII), the silver atoms are all bonded to five oxygen atoms each with initially one short bond [Ag–O(1)] and two pairs of longer bonds [Ag–O(2) and Ag–O(3)]. In this structure in DFT the Ag–O(2) and Ag–O(3) distances become equivalent and only two different distances are distinguished. In DFT + U, we observe two sets of Ag–O distances too, but in this case the Ag–O(1) distance becomes slightly shorter and the other ones become longer. Thus in the optimized cell of structure I, both in DFT and in DFT + U, two types of Ag–O bonds are found, one short and four longs of quite similar lengths, in a square pyramidal environment (Fig. 6).

In structure II (Table VIII), two types of silver atoms are identified. In our calculations, we have estimated the initial atomic positions for this structure from the positions of the $Cu_2V_4O_{11}$ compound, as suggested in Ref. 11. In this compound, two types of Cu atoms exist according to their crystallographic environment.[12] During the cell optimization, we observe that, for SVO, this characteristic is maintained

TABLE VIII. Ag–O interatomic distances for structure II, from cell optimization performed in DFT and DFT + U (U_{eff} = 7.0 eV). All distances are given in Å.

	Exp[a]	DFT	DFT+ *U*
Ag1–O(1)	1.975	–	2.377(×2)
Ag1–O(2)	2.086(×2)	–	2.455(×2)
Ag1–O(3)	2.725(×2)	⟨2.427⟩(×4)	2.474(×2)
Ag2–O(1)	1.928	—	2.278
Ag2–O(2)	1.964	2.304 (×3)	2.380(×2)
Ag2–O(3)	2.035(×2)	2.737	2.586

[a]Because of the lack of precise experimental data for this structure, the interatomic distances have been estimated from those of the $Cu_2V_4O_{11}$ compound, reported by Galy *et al.*,[12] as suggested in Ref. 11.

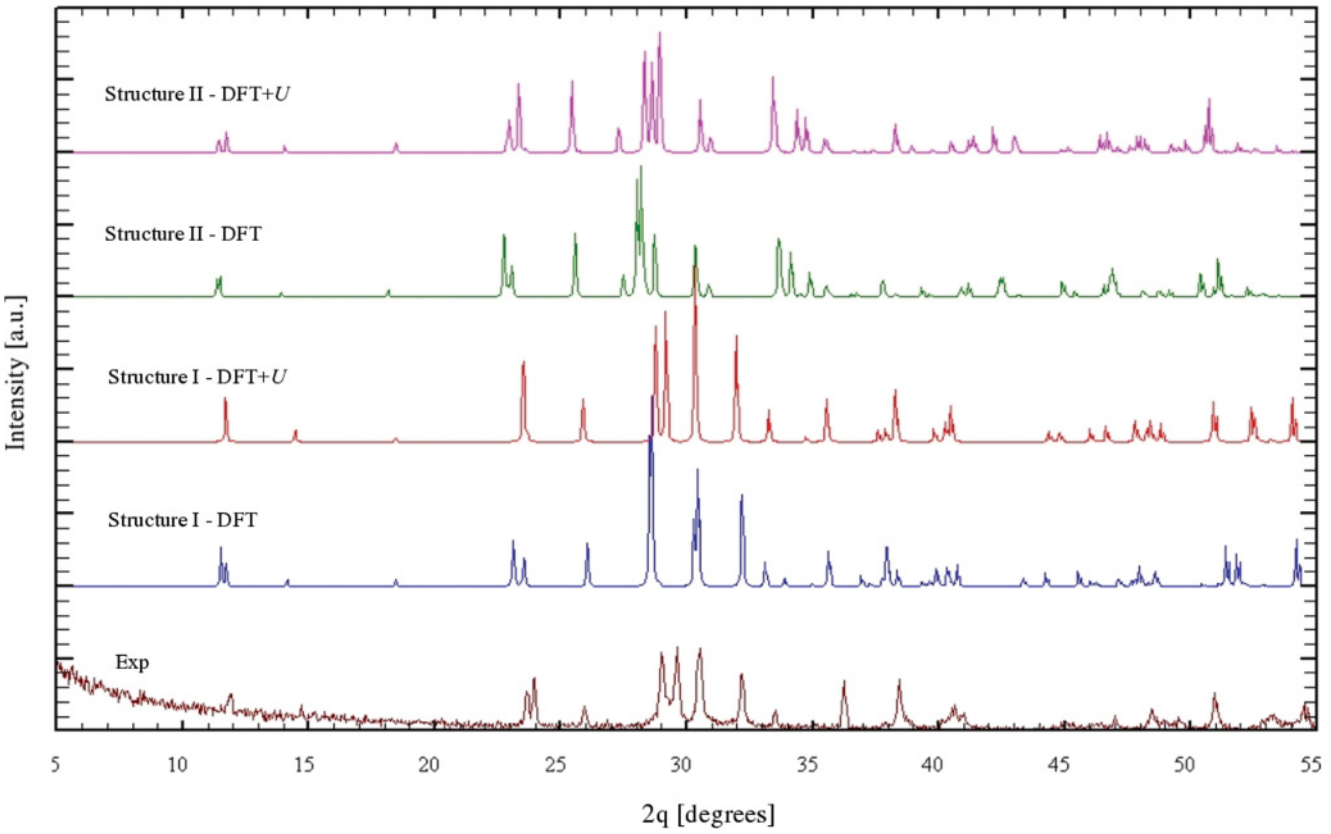

FIG. 7. (Color online) Comparison of the x-ray diffraction spectra of structures I and II of SVO, computed using the Powder Cell software,[63] with the experimental data measured on structure I.

with one type of silver atom bonded to six oxygen atoms (Ag1) and the other type bonded to four oxygen atoms (Ag2), inside a sphere of radius of 2.8 Å. In the DFT calculations, the values of the Ag1–O distances are all different with an average value of 2.427 Å, whereas for Ag2 we find three distances around 2.30 Å and one distance at 2.737 Å. The situation changes slightly with the use of the Hubbard correction since we observe a structuration of the Ag–O environment. Indeed, the Ag–O1 are now gathered in pairs and Ag1 presents a quasiperfect octahedral environment. For Ag2, we observe a tetrahedral environment with one short bond, two equal bonds and one long bond (Fig. 6).

From our calculations, we can conclude that the two structures I and II are quite different. Firstly the β angle is much smaller in structure II than in structure I, and secondly the layers along the z direction are stacked differently in the two structures. X-ray diffraction patterns obtained using the optimized cell parameters have been computed using the Powder Cell software[63] and compared with the experimental one measured on the structure I of SVO (Fig. 7). A comparison of these data allows to directly confirm that structures I and II are totally different and that the optimized cell of structure I, using DFT + U, is in good agreement with experimental data.

3. *Electronic structure*

In Fig. 8, we present the total and partial Kohn-Sham densities of states (EDOS) for the optimized cells in DFT and DFT + U for $Ag_2V_4O_{11}$, structures I and II. In both cases, we see from the results presented in Table IV that there is an opening of the electronic gap when the Hubbard correction is applied, as it has already been observed in other similar systems (V_2O_5 and $Li_xV_2O_5$[53] for instance). In Fig. 8 we also observe a widening of the valence band in DFT + U compared to that computed in DFT.

Besides, we also note that, for both structures I and II, the partial Ag 4*d* band is narrower in DFT + U than in DFT. This implies a modification of the valence band which then exhibits a more distinct separation between the Ag 4*d* peaks and the central peaks attributed to hybrid V 3*d*–O 3*p* states, in DFT + U with respect to DFT. Indeed, by adding the U term on the V 3*d* vanadium orbitals, we indirectly make the V 3*d*–O 3*p* bonds more covalent and, at the same time, the Ag–O bonds are weakened. Consequently, the interatomic Ag—-O distances appear longer in DFT + U than in DFT, and the separation between the Ag 4*d* and O 3*p* bands, which are much less hybridized, is more important close to the Fermi level.

Overall the EDOS of the two structures show very similar characteristics which implies that there exist some common structural properties defining these systems, with an important energetic contribution to the valence band: The connectivity of the $[V_4O_{11}]_n$ layers most certainly governs the chemistry of these compounds.

More details can be obtained by looking at the HOMO (Highest Occupied Molecular Orbital) and LUMO (Lowest Unoccupied Molecular Orbital) states for the two optimized structures, with and without the Hubbard correction. Indeed,

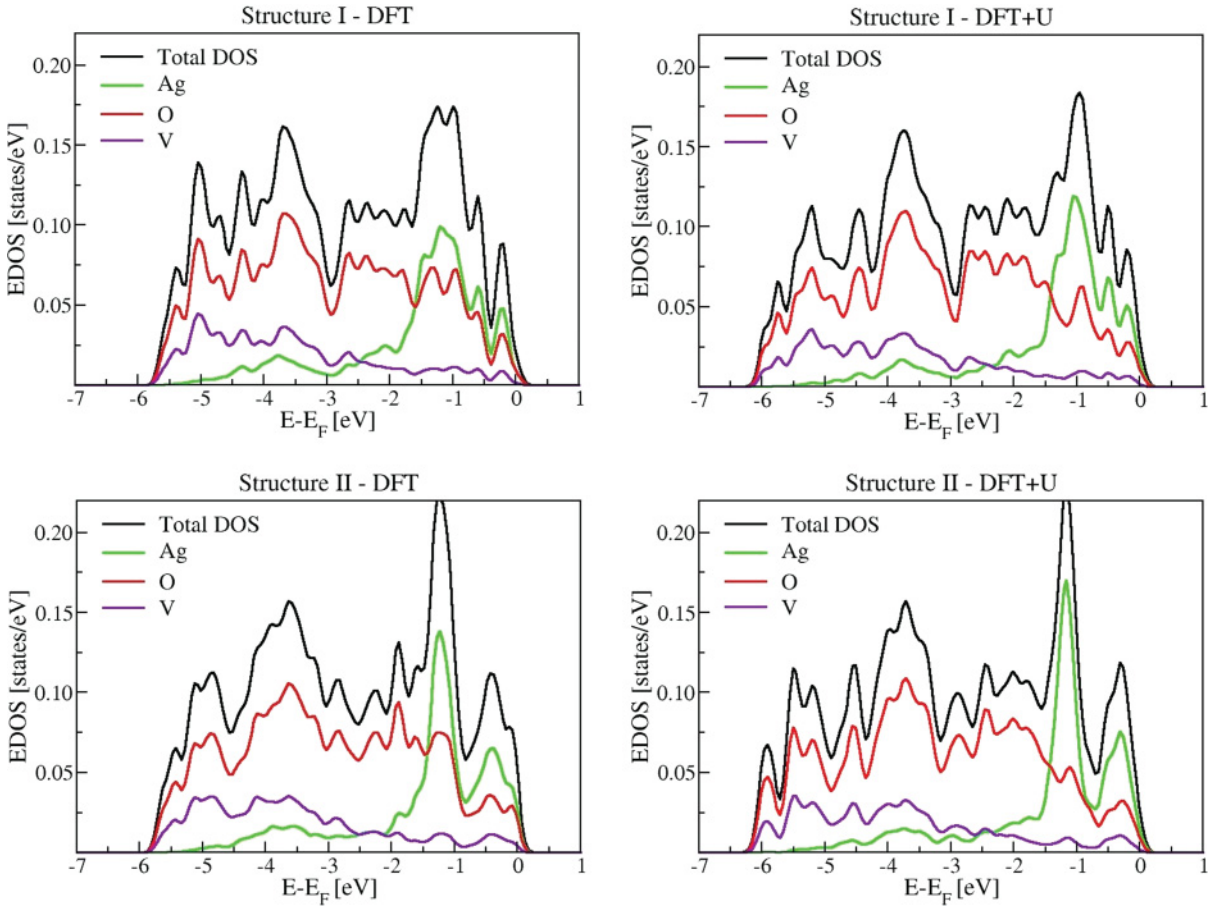

FIG. 8. (Color online) Total and partial Kohn-Sham electronic densities of states for structures I and II, in DFT and DFT + U ($U_{eff} = 7.0$ eV).

an observation of the LUMO states can give valuable insights on the electrochemical behavior of the system, particularly allowing to predict which atomic species would be first reduced in the reaction with lithium. The HOMO and LUMO orbitals

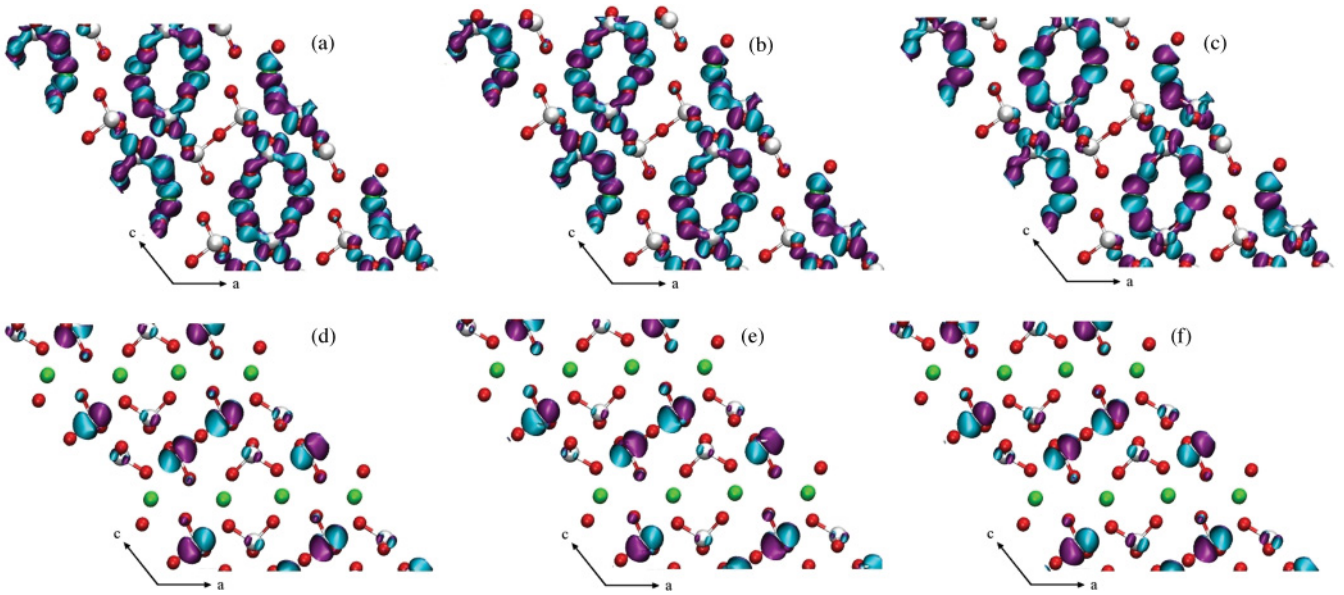

FIG. 9. (Color online) Isosurfaces (0.01 $|e|/Å^3$) of the HOMO (a, b and c) and LUMO (d, e and f) states for DFT and DFT+U ($U_{eff} = 7.0$ eV) calculations of structure I. The (a) and (d) pictures correspond to DFT calculations performed on the fixed experimental cell, the (b) and (e) (respectively (c) and (f)) pictures correspond to DFT (respectively DFT+U) cell optimization calculations.

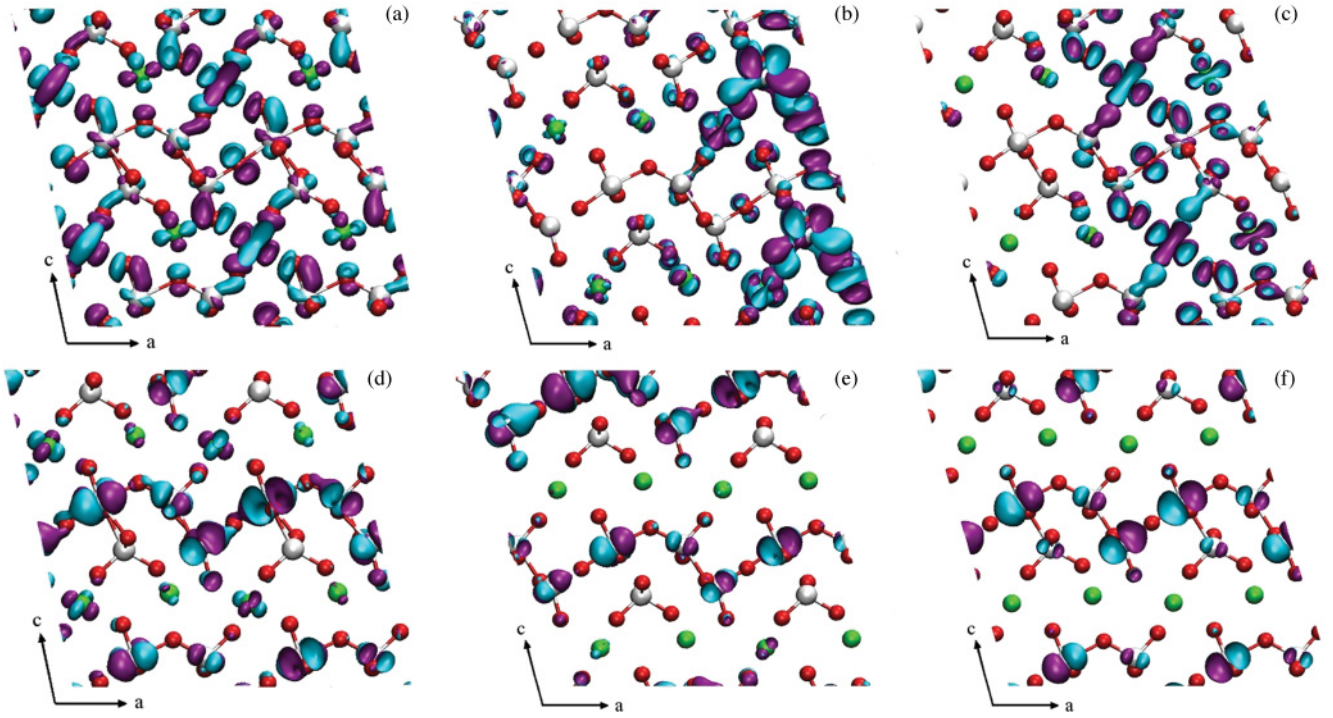

FIG. 10. (Color online) Isosurfaces (0.01 $|e|/Å^3$) of the HOMO [(a), (b), and (c)] and LUMO [(d), (e), and (f)] states for DFT and DFT + U (U_{eff}=7.0 eV) calculations of structure II. (a) and (d) correspond to DFT calculations performed on the fixed experimental cell; (b) and (e) [respectively (c) and (f)] correspond to DFT (respectively DFT + U) cell optimization calculations.

are presented in Figs. 9 and 10 together with those computed for the fixed experimental cell after a geometry optimization.

From Fig. 9(a), 9(b), and 9(c), one can see that, in structure I, the HOMO exhibits a major contribution from the vanadium atoms of type 2 (V2), through their bonds with the oxygen atoms O1 (vanadyl) and O2' (see Fig. 2). The HOMO has also a contribution from the silver atoms and thus creates a bridge between the V_2O_5 layers through the Ag atoms. On the other hand, for this structure, the LUMO state [Fig. 9(d), 9(e), and 9(f)] is mainly localized on vanadium atoms of type 1 (V1). The HOMO and LUMO states for structure I remain almost unchanged after the cell optimization and are similar in DFT and DFT + U. This result indicates that for this system the structural modifications observed during the cell optimization do not affect the electronic properties of the system close to the Fermi level.

In structure II, the LUMO state [Fig. 10(d), 10(e), and 10(f)] presents the same characteristics to that of structure I: It is mainly localized on the V1 atoms. However, in contrast to what is observed for structure I, the cell optimizations in DFT and in DFT + U lead to important modifications in the HOMO state [Figs. 10(a), 10(b), and 10(c)]. After the cell optimization in

TABLE IX. Mülliken and Bader charges of the different atom types, in structures I and II, after cell optimization in DFT and DFT + U (U_{eff} = 7.0 eV). The atomic labels correspond to those presented in Fig. 2, the number in parenthesis indicating the vanadium type for the vanadyl oxygens. For the Ag atoms in structure II, the type is indicated in parentheses (see Fig. 6).

	Structure I				Structure II			
	Mulliken		Bader		Mulliken		Bader	
	DFT	DFT + U	DFT	DFT + U	DFT	DFT + U	DFT	DFT + U
Ag	0.646	0.590	0.792	0.776	0.612(1)	0.584(1)	0.770(1)	0.743(1)
					0.672(2)	0.623(2)	0.834(2)	0.827(2)
V1	0.804	1.204	2.102	2.314	0.825	1.223	2.079	2.332
V2	0.767	1.170	2.047	2.276	0.813	1.196	2.059	2.300
O1(1)	−0.259	−0.360	−0.716	−0.780	−0.308	−0.401	−0.742	−0.804
O1(2)	−0.339	−0.434	−0.804	−0.863	−0.350	−0.446	−0.792	−0.853
O2	−0.366	−0.527	−0.868	−0.929	−0.350	−0.525	−0.871	−0.976
O2	−0.453	−0.568	−0.928	−0.999	−0.449	−0.569	−0.922	−1.015
O3	−0.474	−0.652	−0.990	−1.096	−0.475	−0.651	−0.983	−1.089
O4	−0.508	−0.687	−1.069	−1.164	−0.523	−0.693	−1.067	−1.167

DFT, the HOMO is quite asymmetric, localized on some of the V2 atoms and with a small contribution from the silver atoms. In DFT + U, the HOMO becomes more symmetric and the connection between the V_2O_5 layers through the silver atoms is recovered, as in structure I. It is interesting to note that the HOMO obtained after cell optimization in DFT + U resembles that obtained for the fixed experimental cell. The important structural changes observed during the cell optimization have here important consequences on the electronic structure of the system. The most important change between the optimized cells in DFT and DFT + U takes place in the modifications of the **a** cell parameter and the β angle. One can then assume that, in this structure, the interactions along the x direction and/or the stacking of the layers in the direction of the **c** cell parameter are crucial for the description of the system.

The fact that the LUMO states, in all the studied cases, show an important contribution coming from the V1 atoms suggests that these atoms could serve as electron acceptor due to lithium insertion during the electrochemical reaction in a battery. This is supported by the fact that the average charge on the V1 vanadium atoms, obtained either from a Mülliken or from a Bader[64,65] analysis, is more positive than that on the vanadium V2 atoms, for both structures in DFT and DFT + U (Table IX). This result is in full agreement with recently published experimental facts[15] indicating that vanadium reduction takes place before silver reduction in the Li + $Ag_2V_4O_{11}$ reaction. We can even predict that this vanadium reduction would start by the V1 atoms.

From Table IX, we can also note that the Hubbard correction leads to a charge transfer from the vanadium atoms toward the oxygen atoms, which was expected due to the V 3*d* orbitals localization induced by U. Consequently the silver atoms have a slightly more negative charge with respect to the DFT calculations. The fact that the absolute values of the charges are different in the Mülliken and Bader analysis is due to a different partitioning of the charge density, which is more appropriate and less arbitrary in the Bader case. However we observe the same trends with both methods.

The charges on the oxygen atoms vary depending on their coordination: As the oxygen has more bonds, its charge is more negative. This tendency is related to the V–O distances: The shorter the V–O distance, the less negative the oxygen charge (the bond is more covalent). Finally, even if the vanadium atoms present slightly different charges, these are coherent with a single valence state for all the V atoms. Indeed, the population of the vanadium 3*d* states in each case (not shown here) corresponds to the V^{5+} state, as expected for this stoichiometry.

IV. CONCLUSIONS

We have presented a detailed study of the $Ag_2V_4O_{11}$ compound which has, to our knowledge, never been investigated theoretically despite its common use as a cathode for high-rate primary lithium batteries and its excellent electrochemical performance. We have developed a simulation protocol based on the study of the system size effects and the effects of the U correction on both the structural and electronic properties of this system.

We have found that a correct theoretical description of the structure of this compound can be obtained by treating the electronic correlation by means of the DFT + U method, in which the U correction is applied to the vanadium 3*d* orbitals. An optimal value of 7.0 eV for U_{eff} has been obtained empirically based on the best description of the structural characteristics of the system. Even if this value is larger than that used in other systems of the vanadium oxide family, for our particular calculation setup, this value has shown to be consistent for the studied structures and has allowed us to obtain results in agreement with experimental data. Our results, both in DFT and DFT + U, show that one of the proposed structure for $Ag_2V_4O_{11}$ in the literature is unstable[11] whereas the other two[11,13] seem to be equally probable. In our simulation, structure II appears to be a hypothetic structure with structural characteristics similar to that of analogous existing compounds, such as $Cu_2V_4O_{11}$, which show interesting electrochemical behavior in the reaction with lithium. However, since this structure has been observed only once and in very specific experimental conditions, the question of its synthesis is still open. More insight could be obtained from *ab initio* molecular-dynamics simulations, from which we could observe the effect of temperature on the relative stability of these two structures.

Finally, from the analysis of the LUMO state, we are able to confirm the proposition of Sauvage *et al.*[15] regarding the earlier stages of the reaction, during lithium insertion and deinsertion in Li/SVO batteries: The reduction of the V^{5+} should take place before that of Ag. Moreover we can specify that this reduction will concern one type of vanadium atoms first, since the LUMO is mainly localized on the V1 atoms. This important result demonstrates the ability of such theoretical investigations to predict the underlying mechanisms in complex redox reactions of this kind. In order to complete the proposed scenario for the lithium insertion in SVO, simulations of $Li_xAg_2V_4O_{11}$ by means of the DFT + U approach will be presented in a forthcoming paper.

ACKNOWLEDGMENTS

We wish to thank Joost van de Vondele and Juerg Hutter for helping us setting up the calculations with CP2K . We also thank Mickaël Dollé and Joseph Morillo from CEMES, and Rafael Almeida from Universidad de Los Andes, for very fruitful discussions. This work was performed using HPC resources from GENCI-CINES (Grant No. 2010-096039) and from CALMIP (Grant No. 2010-p0907). M.G. thanks the Universidad de Los Andes for financial support.

[1] J. M. Gallardo Amores, N. Biskup, U. Amador, K. Persson, G. Ceder, E. Morán, and M. E. Arroyo y de Dompablo, Chem. Mater. **19**, 5262 (2007).

[2] K. J. Takeuchi, A. C. Marschilok, S. M. Davis, R. A. Leising, and E. S. Takeuchi, Coord. Chem. Rev. **219**, 283 (2001).

[3] E. S. Takeuchi and R. A. Leising, MRS Bull. **27**, 624 (2002).

[4]R. A. Leising, W. C. Thiebolt III, and E. S. Takeuchi, Inorg. Chem. **33**, 5733 (1994).
[5]R. P. Ramasamy, C. Feger, T. Strange, and B. N. Popov, J. App. Electrochem. **36**, 487 (2006).
[6]S. Beninati, M. Fantuzzi, M. Mastragostino, and F. Soavi, J. Power Sources **157**, 483 (2006).
[7]S. Zhang, W. Li, C. Li, and J. Chen, J. Phys. Chem. B **110**, 24855 (2006).
[8]Z. Chen, S. Gao, R. Li, M. Wei, K. Wei, and H. Zhou, Electrochim. Acta **53**, 8134 (2008).
[9]K. J. Takeuchi, R. A. Leising, M. J. Palazzo, A. C. Marschilok, and E. S. Takeuchi, J. Power Sources **119**, 973 (2003).
[10]J. Kawakita, K. Makino, Y. Katayama, T. Miura, and T. Kishi, J. Power Sources **75**, 244 (1998).
[11]H. W. Zandbergen, A. M. Crespi, P. M. Skarstad, and J. F. Vente, J. Solid State Chem. **110**, 167 (1994).
[12]J. Galy and D. Lavaud, Acta Crystallogr. B **27**, 1005 (1971).
[13]M. Onoda and K. Kanbe, J. Phys. Condens. Matter **13**, 6675 (2001).
[14]A. M. Crespi, P. M. Skarstad, and H. W. Zandbergen, J. Power Sources **54**, 68 (1995).
[15]F. Sauvage, V. Bodenez, H. Vezin, M. Morcrette, J.-M. Tarrascon, and K. R. Poeppelmeier, J. Power Sources **195**, 1195 (2010).
[16]P. Hohenberg and W. Kohn, Phys. Rev. B **136**, 864 (1964).
[17]W. Kohn and L. Sham, Phys. Rev. A **140**, 1133 (1965).
[18]J. P. Perdew, K. Burke, and M. Ernzerhof, Phys. Rev. Lett. **77**, 3865 (1996).
[19]K. Knížek, P. Novák, and Z. Jirák, Phys. Rev. B **71**, 054420 (2005).
[20]J. VandeVondele, M. Krack, F. Mohamed, M. Parrinello, T. Chassaing, and J. Hutter, Comput. Phys. Commun. **167**, 103 (2005).
[21]J. VandeVondele, M. Iannuzzi, and J. Hutter, Lect. Notes Phys. **703**, 287 (2006).
[22][http://cp2k.berlios.de/].
[23]J. VandeVondele and J. Hutter, J. Chem. Phys. **127**, 114105 (2007).
[24]S. Goedecker, M. Teter, and J. Hutter, Phys. Rev. B **54**, 1703 (1996).
[25]G. Kresse and J. Hafner, Phys. Rev. B **47**, 558 (1993).
[26]G. Kresse and J. Hafner, Phys. Rev. B **49**, 14251 (1994).
[27]G. Kresse and J. Furthmller, Comput. Mat. Sci. **6**, 15 (1996).
[28]G. Kresse and J. Furthmller, Phys. Rev. B **54**, 11169 (1996).
[29]R. Enjalbert and J. Galy, Acta Crystallogr. C **42**, 1467 (1986).
[30]S. F. Cogan, N. M. Nyugen, S. J. Perroti, and R. D. Rauh, J. Appl. Phys. **66**, 1333 (1989).
[31]A. Z. Moshfegh and A. Ignatiev, Thin Solid Films **198**, 251 (1991).
[32]K. P. Huber and G. Herzberg, *Molecular Spectra and Molecular Structure* (Van Nostrand, New York, 1979), Vol. 4.
[33]J. Goclon, R. Grybos, M. Witko, and J. Hafner, J. Phys. Condens. Matter **21**, 095008 (2009).
[34]M. V. Ganduglia-Pirovano and J. Sauer, Phys. Rev. B **70**, 045422 (2004).
[35]T. Kerber, M. Sierka, and J. Sauer, J. Comput. Chem. **29**, 2088 (2008).
[36]S. Grimme, J. Comput. Chem. **27**, 1787 (2006).
[37]E. Londero and E. Schröder, Phys. Rev. B **82**, 054116 (2010).
[38]M. Dion, H. Rydberg, E. Schroder, D. C. Langreth, and B. I. Lundqvist, Phys. Rev. Lett. **92**, 246401 (2004).
[39]M. I. Bertoni, N. J. Kidner, T. O. Mason, T. A. Albretch, E. M. Sorensen, and K. R. Poeppelmeier, J. Electroceram. **18**, 189 (2007).
[40]P. Rozier, J.-M. Savariault, and J. Galy, J. Solid State Chem. **122**, 303 (1996).
[41]B. Raveau, Rev. Chim. Miner. **4**, 729 (1967).
[42]M. Morcrette, P. Martin, P. Rozier, H. Vezin, F. Chevallier, L. Laffont, P. Poizot, and J.-M. Tarascon, Chem. Mater. **17**, 418 (2005).
[43]J. M. Prez-Jord and A. D. Becke, Chem. Phys. Lett. **233**, 134 (1995).
[44]P. Hobza, J. Sponer, and T. Reschel, J. Comput. Chem. **19**, 1315 (1995).
[45]N. Suaud and M.-B. Lepetit, Phys. Rev. Lett. **88**, 056405 (2002).
[46]J. S. Braithwaite, C. R. A. Catlow, J. H. Harding, and J. D. Gale, Phys. Chem. Chem. Phys. **3**, 4052 (2001).
[47]M.-L. Doublet and M.-B. Lepetit, Phys. Rev. B **71**, 075119 (2005).
[48]V. I. Anisimov, J. Zaanen, and O. K. Andersen, Phys. Rev. B **44**, 943 (1991).
[49]V. I. Anisimov, I. V. Solovyev, and M. A. Korotin, M. T. Czyyk, and G. A. Sawatzky, Phys. Rev. B **48**, 929 (1993).
[50]A. I. Liechtenstein, V. I. Anisimov, and J. Zaanen, Phys. Rev. B **52**, R5467 (1995).
[51]S. L. Dudarev, G. A. Botton, S. Y. Savrasov, C. J. Humphreys, and A. P. Sutton, Phys. Rev. B **57**, 1505 (1998).
[52]L. Wang, T. Maxisch, and G. Ceder, Phys. Rev. B **73**, 195107 (2006).
[53]D. O. Scanlon, A. Walsh, B. J. Morgan, and G. W. Watson, J. Phys. Chem. C **112**, 9903 (2008).
[54]Z. S. Popović and F. R. Vulkajlović, J. Phys. Soc. Japan **71**, 2720 (2002).
[55]M. Yashima and R. O. Suzuki, Phys. Rev. B **79**, 125201 (2009).
[56]J. L. F. Da Silva, M. V. Ganduglia-Pirovano, and J. Sauer, Phys. Rev. B **76**, 125117 (2007).
[57]V. I. Anisimov, D. M. Korotin, S. V. Streltsov, A. V. Kozhevnikov, J. Kuneš, A. O. Shorikov, and M. A. Korotin, JETP Lett. **88**, 729 (2008).
[58]C. Tablero, J. Phys. Condens. Matter **20**, 325205 (2008).
[59]N. Stojić, N. Binggeli, and M. Altarelli, Phys. Rev. B **73**, 100405(R) (2006).
[60]M. Calatayud and C. Minot, J. Phys. Chem. C **111**, 6411 (2007).
[61]A. N. Yaresko, V. N. Antonov, H. Eschrig, P. Thalmeier, and P. Fulde, Phys. Rev. B **62**, 15538 (2000).
[62]P. Rozier, M. Dollé, and J. Galy, Journal of Solid State Chemistry France **182**, 1481 (2009).
[63]W. Kraus and G. Nolze, J. Appl. Cryst. **29**, 301 (1996).
[64]R. Bader, *Atoms In Molecules: A Quantum Theory* (Clarendon Press, Oxford, 1990).
[65]G. Henkelman, A. Arnaldsson, and H. Jónsson, Comput. Mater. Sci. **36**, 254 (2006).